



United States Department of Commerce
Technology Administration
National Institute of Standards and Technology

NIST Special Publication 919

*International Workshop on Fire Performance
of High-Strength Concrete, NIST,
Gaithersburg, MD, February 13-14, 1997
Proceedings*

Long T. Phan, Nicholas J. Carino, Dat Duthinh, and Edward Garboczi



B.6 An Analytical Approach for Investigating the Causes of Spalling of High-Strength Concrete at Elevated Temperatures

Gamal N. Ahmed and James P. Hurst

Portland Cement Association
5420 Old Orchard Road,
Skokie, IL 60077-1083

Background

Explosive spalling of high-strength concrete (HSC) elements and cylinder specimens has occurred unpredictably and on an inconsistent basis during laboratory fire tests. Differences in the structural fire performance of specimens constructed of HSC versus normal-strength concrete (NSC) have been attributed to differences in the mechanical properties of the two types of concretes at elevated temperatures. Because of these differences, structural design provisions for NSC may not be applicable to HSC for use in structures required to be fire resistance rated. The inconclusive nature of fire tests involving HSC columns suggests that additional research is needed, not only to gain a better understanding of the cause or causes of spalling, but to obtain a clearer picture of the fire performance of HSC structural members in general.

Purpose

This paper will primarily focus on the issue of spalling. The objectives are as follows: to present an overview of the performance inconsistencies of HSC at elevated temperature based on laboratory fire tests of HSC columns; to propose an analytical approach for investigating the cause or causes of spalling; and to recommend work that is needed in support of the analytical study.

Behavior of high strength concrete exposed to fire

Results from research projects sponsored by the Portland Cement Association (PCA) and others involving fire tests of HSC have shown that the material performs significantly differently under fire exposure than does NSC. Table 1 provides column specifications and other pertinent information for 3 carbonate aggregate, 406 mm x 406 mm HSC columns that were tested at the National Research Council of Canada test facility. Fig. 1 shows the temperature history results from the 3 fire tests. Thermocouple measurements were taken at distances normal to the surface and along the centerline of each column.

Table 1. Concrete Mixtures for HSC column fire test specimens

Column designation	Column HS-1	Column HS-2	Column HS-4
Test date	11-4-94	7-3-96	6-19-96
Cement type I, lb (kg)	800 (362.8)	820 (371.8)	653 (296.1)
Coarse agg., SSD*, lb (kg)	1800 (816.3)	1800 (816.3)	1563 (708.8)
Aggregate type	carbonate	carbonate	carbonate
Water cement ratio	0.338	0.320	0.395
Water cementitious material ratio	0.287	0.291	0.359
% Silica fume:cement	5.00	9.76	9.95
% Fly ash:cement	12.50	0.0	0.0
Cylinder strength, ksi (MPa)	14.5 (100.0)	18.35 (126.5)	12.7 (87.6)

* SSD is saturated surface dry condition.

Although the columns were all made with the same aggregate and cast at the same time, Column HS-1 was tested 19-20 months earlier than HS-2 and HS-4. Of the three columns, the shorter drying period of HS-1, and thus, its higher initial moisture content, typically would have been expected to produce the lowest data readings for temperature history. This is clearly not the case, however, as Fig. 1 shows just the opposite is true. Aside from the influence of drying time, all three columns contained the same aggregate type, and therefore, should have had similar thermal conductivity properties. Since thermal conductivity has the most dominant influence on temperature profile, it would be expected that the data from the 3 column tests should reflect close agreement in temperature histories. Again, this was not the case. These expectations would have held true had the columns been produced with normal strength concrete. The inconsistencies in fire performance of these HSC specimens from the anticipated behavior make the results of such testing inconclusive at best.

Fig. 2 compares the PCA heat and mass transfer model predictions of temperature history against the data from HS-1. Column HS-1 was selected for validation purposes because it was the only column specimen tested in an unloaded condition. One can see from the figure that the agreement between model results and test data is good.

In an attempt to force the model predictions into agreement with the lower temperature histories of the other two columns, computer runs were performed using artificially low and unrealistic thermal conductivity relationships as input data. These efforts, however, proved unsuccessful, as it was impossible to bring the curves down to the levels indicated by the test data. The fact that the experimental temperature curves are not consistent with physical laws

indicates a problem for which there is no explanation at present. Again, these types of inconsistencies support the need for additional research.

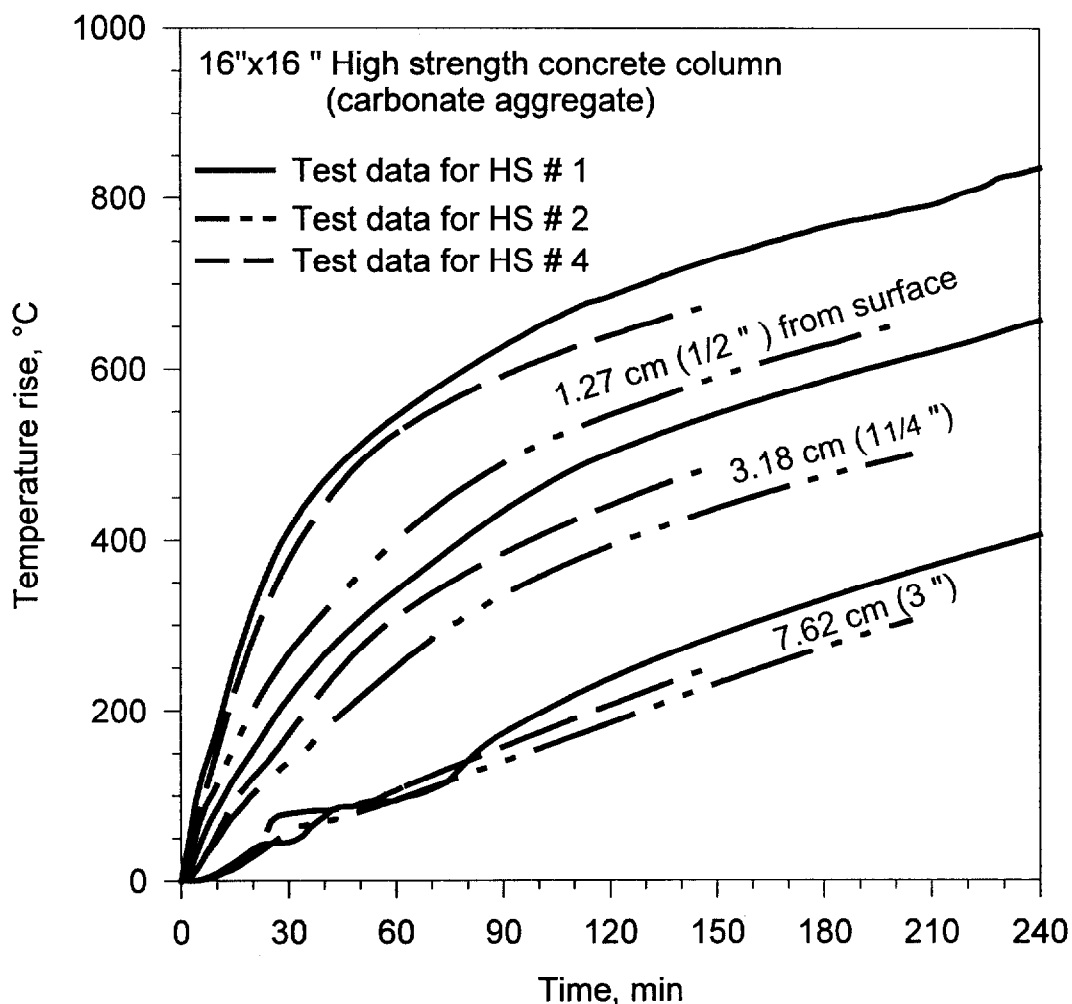


Figure 1. Temperature history data for columns HS # 1, 2, and 4 subjected to ASTM E 119 fire.

Potential causes of spalling

Over the years, several explanations have been offered regarding the primary cause of concrete spalling at elevated temperature. Spalling has been attributed to thermal stresses due to temperature gradient, as well as thermal expansion of unlike materials such as concrete and reinforcing steel. Excessive loading or inadequate reinforcement has also been suggested as the source of spalling. In other theories, pore pressure buildup has been said to have the greatest influence. In fact, the spalling phenomenon is likely to be caused by the cumulative effect of all of these factors. With respect to which one plays the dominant role, the authors' beliefs are

aligned with those of the pore pressure perspective. This perspective is based on the following discussion.

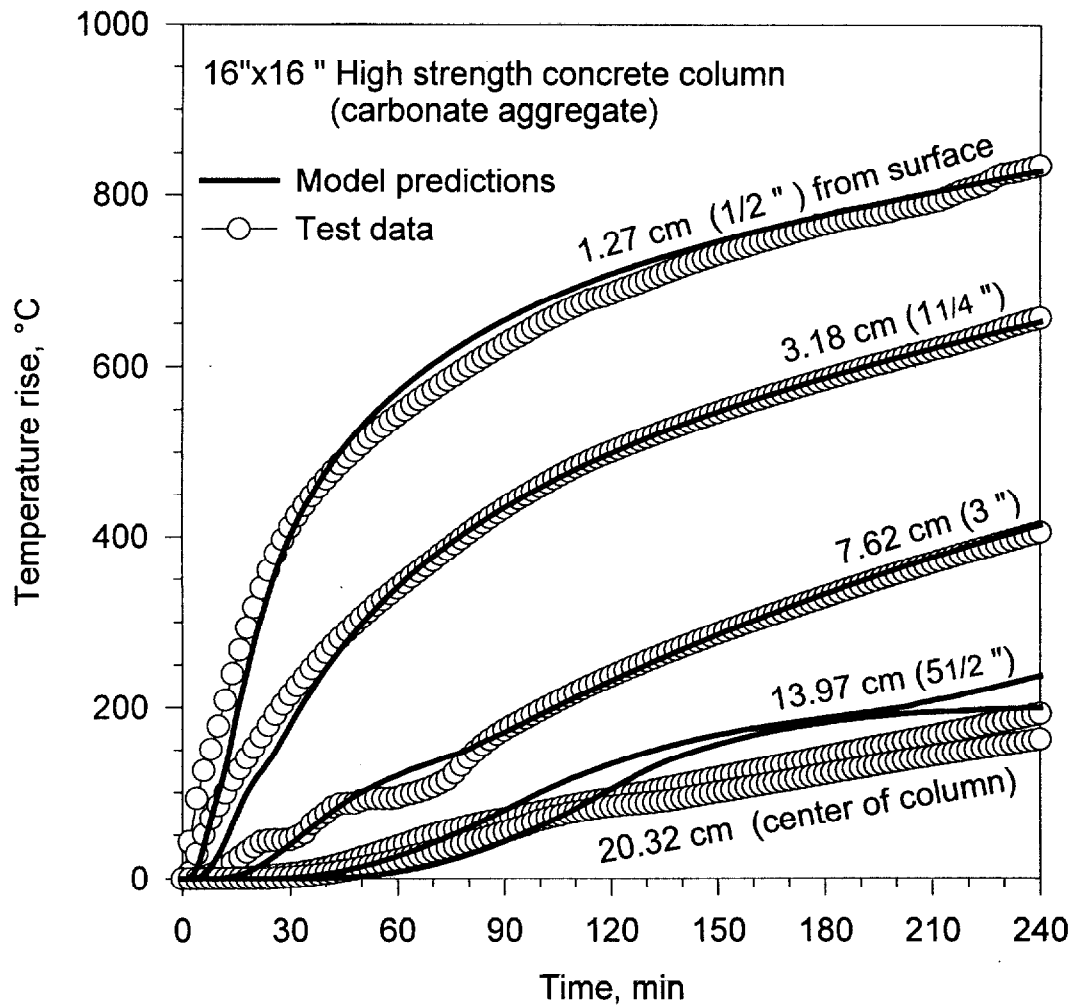


Figure 2. Comparison of the predicted temperature history of column HS # 1 against ASTM E 119 fire test data.

Researchers who have suggested thermal stresses as the primary cause of spalling, generally dismiss the effects of pore pressure as negligible. If thermal stresses were truly the governing factor, however, then NSC of a given aggregate type would likely be susceptible to the same type of spalling problems as its HSC counterpart due to similarities in their thermal conductivities. Contrarily, this behavior has not been evident from field experience, and the issue of spalling associated with structural members constructed of normal strength concrete has not warranted cause for concern.

Others have felt that the spalling of high-strength concrete at elevated temperature is more of a structural problem than a fire problem. If this were true, then concretes used in unloaded applications, such as refractory concretes for furnace liners, would not be expected to have spalling problems. This, of course, is not the case, as spalling is very much a concern for concretes exposed to high-temperature environments. In practice, the standard method that is used to eliminate spalling is to pre-condition the concretes through a specialized drying process. Removing the moisture reduces the possibility of pore pressure build up.

Furthermore, it is widely known that the addition of polypropylene fibers has been successful in reducing the spalling problem in HSC member subjected to fire. Again, if spalling were primarily the result of loading conditions or thermal effects, there is no reasonable explanation as to why this technique would have succeeded. Melting and/or shrinkage of fibers at elevated temperature increases concrete permeability, which is shown to have a strong influence on pore pressure buildup (see Fig. 8). The fact that the addition of fibers has proven successful in alleviating spalling is a solid testament that pore pressure plays a significant role in the occurrence of spalling. To date, this assertion is primarily qualitative. The section that follows offers a methodology that will lead to a quantitative resolution of this.

Proposed approach for investigating the cause of spalling

The question of degree of influence of the factors that may contribute to spalling can only be answered through a robust analytical procedure involving parametric studies and a stress analysis. The proposed approach for the stress analysis (for a member subjected to a standard fire test) is to determine the total stress at a given depth due to thermal gradient, thermal expansion, load, pore pressure, etc., and compare it with the heat-reduced strength of the material at a desired time.

Possibly, the most reasonable and efficient way of achieving this is to merge an appropriate thermal model with a compatible structural analysis model. The heat and mass transfer model discussed in this paper serves well in this capacity because of its relatively unique capability of predicting pore pressure, which is identified as a critical factor in the spalling process. In addition, the model provides temperature history results that are necessary for determining the change in the material's temperature-dependent mechanical properties. Parametric studies of parameters affecting pore pressure can also be done with the model, and some examples of these are presented later in this paper.

Synopsis of the model

As a precursor to the parametric examples, a brief synopsis of the model is given with respect to some of its characteristics, assumptions, and considerations. An explanation of the coupling relationship between temperature, moisture content, and pore pressure histories and distributions is also presented. Detailed information about the model is provided in Refs. 1, 2, and 3.

Model characteristics

Some of the primary characteristics of the model can be summarized as follows:

- heat and mass transport phenomena are coupled
- conservation of mass, momentum, and energy equations coupled to constitutive relations of the material drive the model
- the model works with any specified heat source
- the model handles various geometries for one- and two-dimensional heat and mass transfer
- model output includes moisture content, pore pressure, and temperature distributions and histories

Model assumptions and considerations

Some of the main model assumptions and considerations are summarized as follows:

- local equilibrium moisture content is related to the relative vapor pressure and temperature using sorption isotherms
- physical and thermal properties of concrete are functions of temperature, pore pressure, and moisture content
- conductive and radiative heat, and mass and heat transfer by convection and diffusion are considered
- evaporation/condensation and dehydration phenomena and their effect on the material pore size are considered
- convective heat and mass transfer are driven by pore pressure gradients
- diffusive transport is driven by mass concentration gradients
- conductive heat transfer is driven by temperature gradients

Coupling relationship

One of the most important attributes of the model is the coupling relationship previously mentioned. Figs. 3, 4, and 5 show the model's predictions of temperature, moisture content, and pore pressure distributions, respectively, for 406 mm x 406 mm carbonate aggregate HSC column, and are used to illustrate this relationship. The depths indicated in the figures represent distances along the diagonal of the cross section.

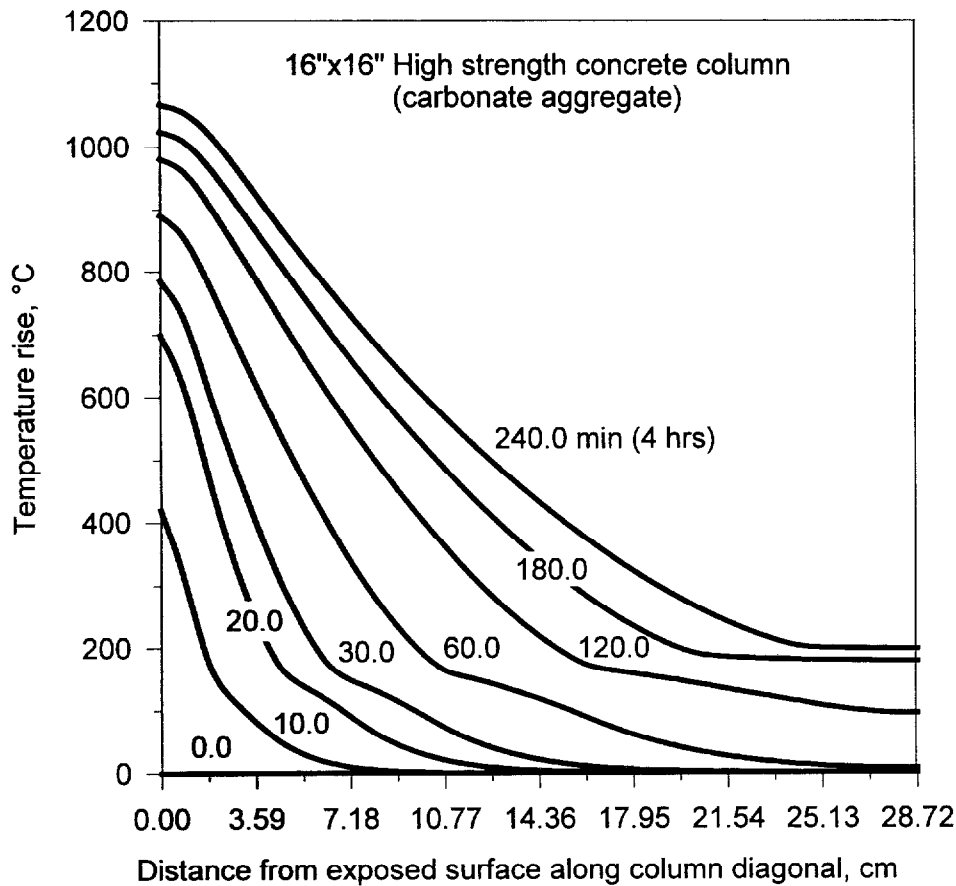


Figure 3. Model-predicted temperature distribution at various times of HSC column subjected to ASTM E 119 fire.

Before getting into the coupling discussion, a brief description of the heat and mass transport phenomena is provided. When a depth of concrete becomes sufficiently hot, the evaporation of the free moisture and chemically bound water takes place. As the water evaporates, pore pressure builds up driving some of the gaseous mixture of air and water vapor toward the column surface. The rest is driven into cooler zones toward the center of the column where it condenses and accumulates as liquid. This accumulation can often exceed the initial moisture content, as seen in Fig. 4. Continued application of heat in the presence of moisture continues to build pore pressure, which in turn, repeats the process of moisture transport followed by moisture condensation and accumulation. This interdependent cycle is repeated until either all of the moisture is gone or the heat source is removed.

In Fig. 3 at 20 minutes, the evaporation process is occurring at a depth of about 72 mm from the fire-exposed surface (where the concrete temperature is at or above 100 °C). In Fig. 4 at this depth and time, the moisture content of the concrete is almost at its initial value because virtually no dehydration of the chemically bound water has yet occurred. It follows from the relatively low temperature at this depth that the pore pressure would also be low under these conditions, and this is confirmed in Fig. 5.

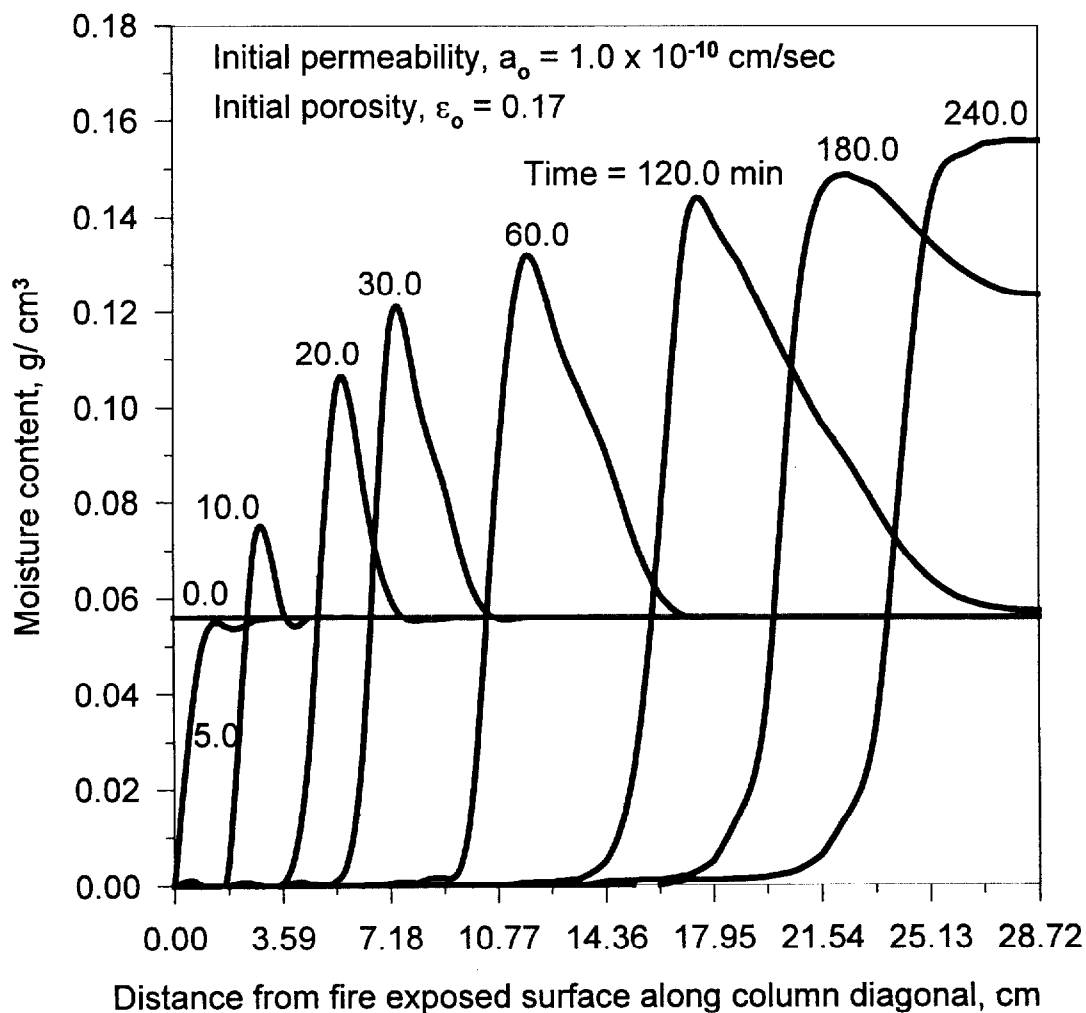


Figure 4. Model-predicted moisture content distribution at various times of HSC column subjected to ASTM E 119 fire.

From Fig. 4 at 20 minutes, the concrete reaches its maximum moisture content at a depth of 54 mm and becomes dry at 36 mm. This portion of the curve (from maximum moisture content to

zero) represents the evaporation front or zone experiencing the highest rate of evaporation. In cross referencing this to Fig. 3, the slope of the temperature curve at 54 mm is moderate, reflecting the moisture's ability to absorb heat as it evaporates. Closer to the surface, where the available moisture has diminished (Fig. 4), the amount of heat that can be absorbed also becomes less. This is reflected by a corresponding increase in steepness of the temperature rise curve in Fig. 3. At 36 mm, where the drying front is located, there is no available moisture to further retard the rate of temperature rise. This is confirmed in Fig. 3 by the sharp increase in temperature rise that is seen in the region bounded by the drying front and the fire-exposed surface of the column.

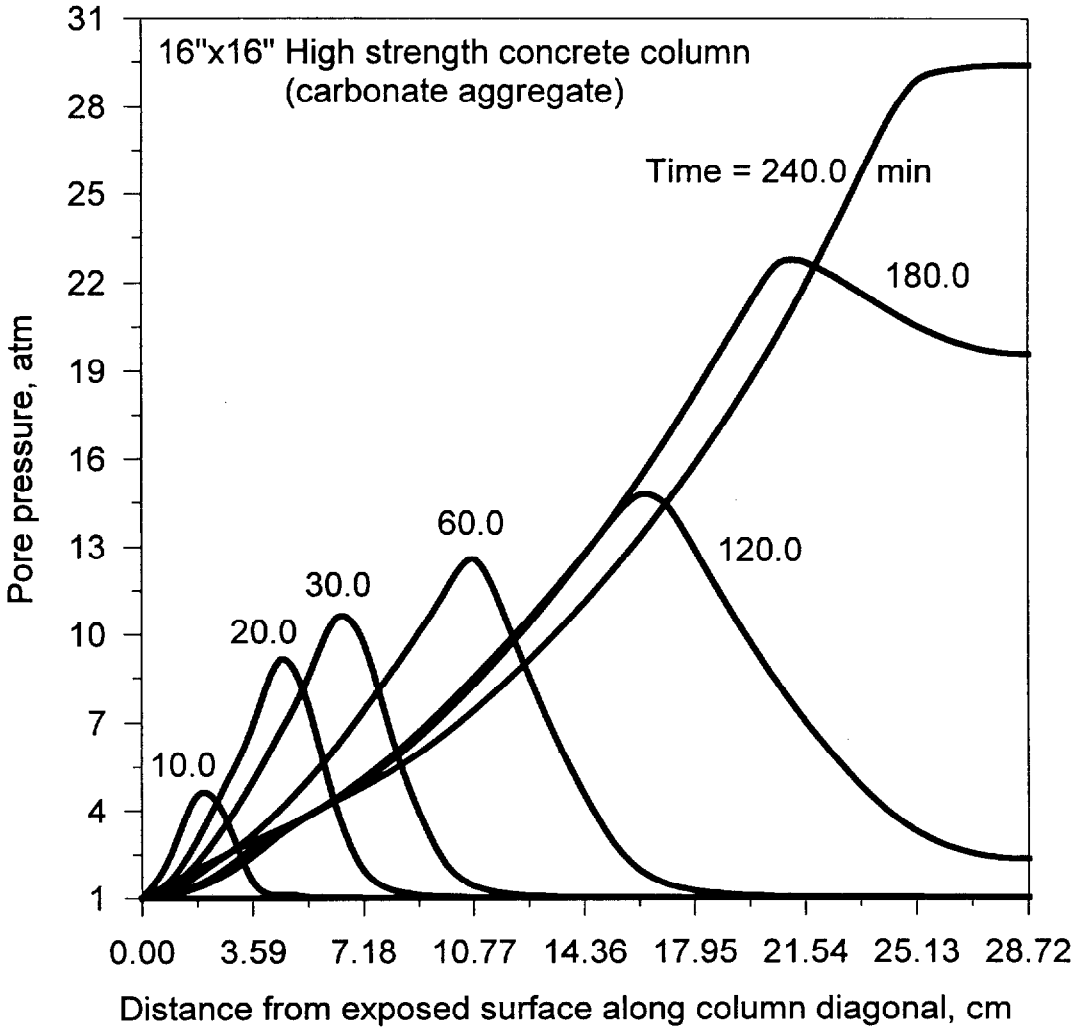


Figure 5. Model-predicted pore pressure distribution at various times of HSC column subjected to ASTM E 119 fire.

In looking at Fig. 5, the peak pore pressure at 20 minutes occurs at a depth somewhere along the evaporation front. In general, as the pore pressure builds, the evaporation front moves toward the center of the column. The pore pressure and moisture content peak at different depths for a given time. At a given time, the pore pressure reaches its maximum value closer to the surface as it continues to force the moisture deeper within the column. At the depth of maximum moisture content, the pore pressure has dropped from its peak value due to lower temperatures that are insufficient to sustain its buildup.

With respect to the temperature associated with the point of maximum pore pressure at 20 minutes, Fig. 3 shows this to be at or near the temperature just prior to where the curve experiences its sharpest change in temperature rise. This is logical, since it corresponds to a region of high evaporation, preceding the elimination of moisture and resulting in the rapid temperature rise.

In cooler zones where no moisture has accumulated, for example, at 20 minutes and depths beyond 90 mm (Fig. 4), corresponding to a temperature of about 50 °C (Fig. 3), the pore pressure is essentially atmospheric. This is reasonable in consideration of almost ambient conditions, and once again, confirms the coupled or dependent relationship of the pore pressure, moisture content, and temperature.

From a physical standpoint, fairly drastic changes are occurring within the column at the 20-minute mark between the depths of 36-72 mm. Since this is a common range of thickness in which spalling occurs, it is no coincidence that spalling has been observed in fire tests of HSC within the 20-30 minute time frame. As an aside, the pore pressure will reach its maximum value at the center of the column (287 mm) if the application of heat continues long enough. This trend is evident in Fig. 5 by the curve representing 240 minutes.

Parametric studies

In order to gain a better understanding of the parameters that affect pore pressure buildup and therefore, spalling potential, the model can be used to perform parametric studies. This is significant, in that a desired behavioral response may be able to be controlled or produced at the mix design stage if the phenomenon in question is sufficiently understood. Figs. 6-8 provide model output from parametric investigations that have been done for a 406 mm x 406 mm carbonate aggregate HSC column. For Fig. 6, the depths are measured along the column centerline normal to the surface. In Figs. 7 and 8, depths represent distances along the diagonal of the column.

Fig. 6 shows model predictions of the effect of initial moisture content on temperature history compared with the data for Column HS-1. The curves indicate that increases in initial moisture content result in lower temperature histories. This is reasonable since higher moisture levels are capable of absorbing more heat.

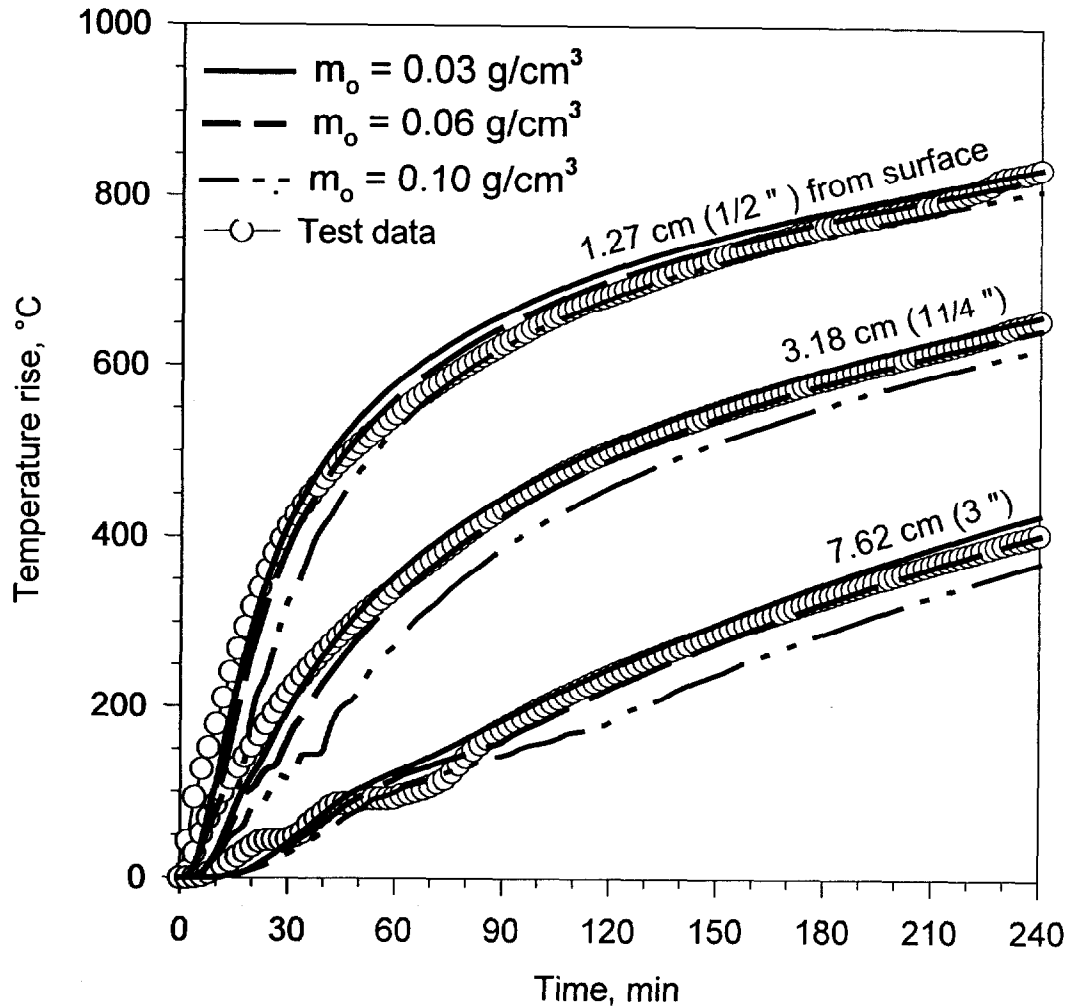


Figure 6. Model-prediction of effect of initial moisture content on temperature history of column HS # 1 compared with E 119 fire test data.

Fig. 7 illustrates the effect of initial moisture content on the pore pressure distribution. The figure indicates an increase in pore pressure as the initial moisture content is increased.

Fig. 8 shows the effect of initial permeability on the pore pressure distribution and clearly indicates the sensitivity of pore pressure to permeability. As previously mentioned, the ability of polypropylene fibers to increase the permeability of concrete is why they have proven to be effective in reducing the spalling of HSC exposed to fire.

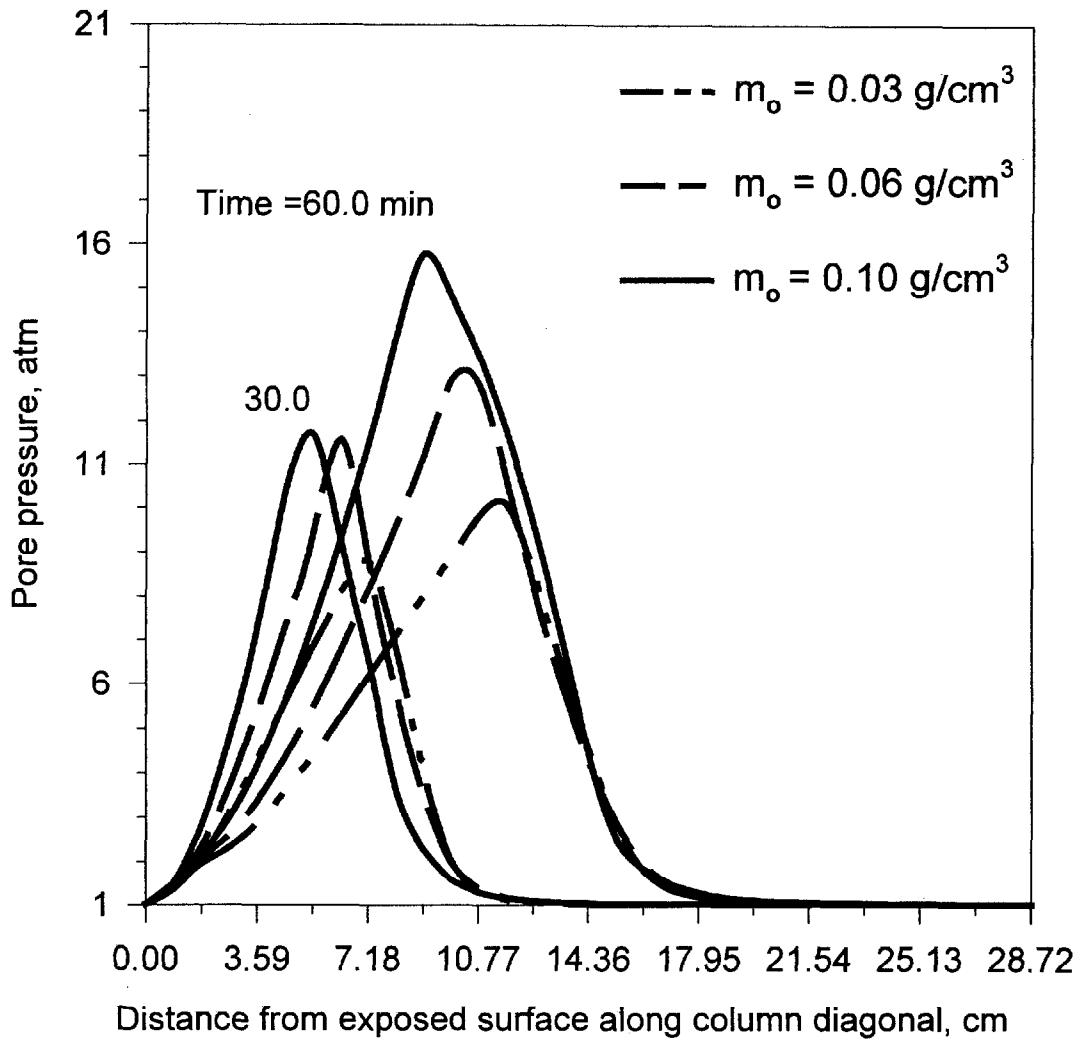


Figure 7. Model-prediction of effect of initial moisture content on pore pressure distribution of 406 mm x 406 mm carbonate aggregate HSC column subjected to E 119 fire.

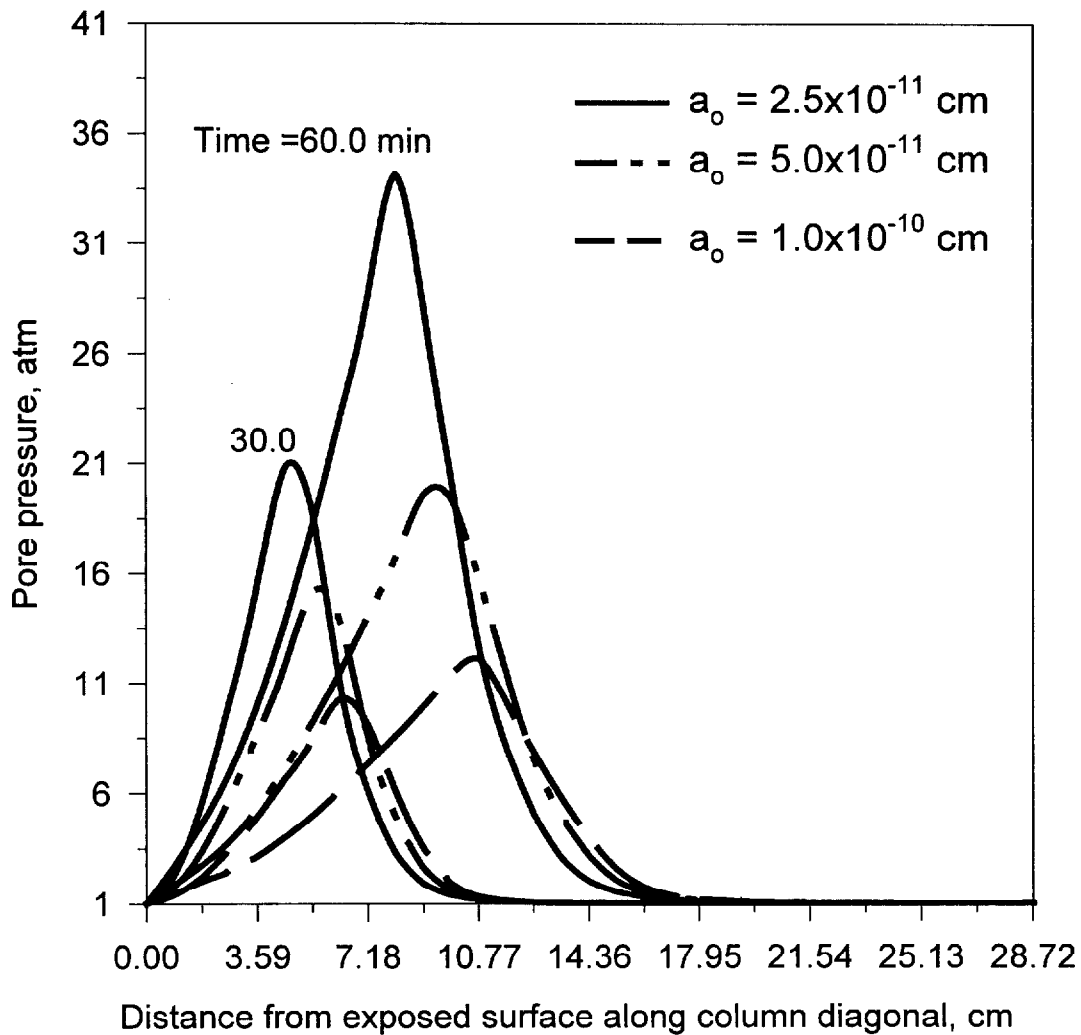


Figure 8. Model-prediction of effect of initial permeability on pore pressure distribution of 406 mm x 406 mm carbonate aggregate HSC column subjected to E 119 fire.

Additional parametric studies are necessary to study the affect of various parameters on HSC fire behavior. These can include the investigation of moisture migration, pore pressure build up, and eventually include the spalling potential and fire performance of HSC. These types of studies are also beneficial in advance of formulating fire test programs for purposes of identifying and eliminating tests that are not expected to yield useful results.

Recommendations in support of the modeling effort

An overall approach for investigating the spalling of HSC under fire conditions has been described. The goal is to develop a computer model that can determine the cause of spalling for purposes of developing a design solution that will eliminate the spalling potential. In order for such an effort to succeed, the following is recommended.

1. Tests involving thermal conductivity, sorption isotherms, permeability, porosity, initial moisture content and others must be performed for high-strength concretes for use as input data.
2. Validation data from full-scale element tests and bench-scale cylinder tests are needed to validate temperature, moisture migration, and pore pressure model predictions.
3. Decisions must be made regarding the merging of a thermal model with a structural analysis model, or whether it is better to start with a thermal model and expand it to include a stress analysis part.

References

1. Gamal N. Ahmed and James P. Hurst, Modeling the Thermal Behavior of Concrete Slabs Subjected to the ASTM E 119 Standard Fire Condition, *Journal of Fire Protection Engineering*, Vol. 7, No. 4, pp. 125-132, Society of Fire Protection Engineers, Boston, MA, 1995.
2. Ali K. Abdel-Rahman and Gamal N. Ahmed, Computational Heat and Mass Transport in Concrete Walls Exposed to Fire, *International Journal of Numerical Heat Transfer, Part A*, Vol. 29, No. 4, pp. 373-395, 1996.
3. Gamal N. Ahmed and James P. Hurst, Coupled Heat and Mass Transport Phenomena in Siliceous Aggregate Concrete Slabs Subjected to Fire, accepted for publication in *International Journal of Fire and Materials*, 1997.